

# The Stability of Euclidean Wormhole Solutions

James Chryssanthacopoulos<sup>1</sup>

<sup>1</sup>University of Padova, Padova PD, Italy

jamespeter.chryssanthacopoulos@studenti.unipd.it

## 1. Introduction

In general relativity, the geometry of spacetime is a dynamic field that changes depending on the matter and energy it contains. Classical solutions to general relativity, wormholes are geometries that connect two asymptotic regions of spacetime [1]. Historically, wormhole solutions arose in the context of black holes, connecting two regions of the spacetime, but wormholes can represent more general geometries. Whatever the kind of wormhole, they are generally not humanly traversable unless supported by some exotic matter field. Although they have been studied for decades, wormholes have received renewed interest because of their role in raising and resolving issues in quantum gravity.

One aspect of quantum gravity that wormholes complicate is the AdS/CFT correspondence. Often viewed as a theory of quantum gravity, the AdS/CFT correspondence establishes a connection between a gravitational system in asymptotically anti-de Sitter space and a conformal field theory defined on its boundary. Specifically, the correspondence equates the sum of all geometries in the gravitational theory to the partition function of the quantum field theory on the boundary. The sum of all geometries is captured by the path integral over all spacetime configurations. This path integral is usually taken over configurations that have a single compact boundary. The challenge arises when the gravitational theory has multiple boundaries, as in the case of wormholes. In that instance, AdS/CFT equates the gravitational theory with distinct quantum field theories over the different boundaries, but the presence of wormholes implies a correlation between these theories that is not accounted for.

A closely related issue that wormholes raise concerns the ability to factor path integrals over geometries with multiple boundaries, depicted in Figure 1. Consider the geometry with a single boundary represented by the first line. Let  $\langle Z \rangle$  be the path integral over all configurations terminating in that boundary. If the geometry is duplicated, as shown on the second line, its path integral should be the product of those of the disconnected geometries,  $\langle Z^2 \rangle = \langle Z \rangle^2$ . The wormhole connecting the boundaries adds a contribution to the path integral that violates this factorization. In the context of AdS/CFT, this inability to factor the path integral means there are correlations between observables on the two boundaries in the gravitational theory, which implies the presence of correlations between the corresponding quantum field theories.

While wormholes challenge the traditional understanding of AdS/CFT, it is unclear the extent to which wormhole solutions contribute to the full calculation of the path integral. The path integral over all geometries is given by

$$Z = \int \mathcal{D}g e^{iS[g]},$$

$$\begin{aligned}
\langle Z \rangle &= \text{[Diagram of a single blue cone-like geometry with two boundaries]} \\
&\neq \left( \text{[Diagram of two separate blue cone-like geometries]} \right) + \text{[Diagram of a red wormhole geometry connecting two boundaries]} \\
&= \langle Z^2 \rangle
\end{aligned}$$

**Figure 1. The path integral over all geometries with two boundaries does not factorize if a wormhole connecting the boundaries is present. This figure is adapted from [2].**

where  $g$  is the metric tensor and  $S[g]$  is the action functional of the theory for a given metric. Since the exponential is an oscillating function, it is common to perform a Wick rotation, introducing the Euclidean time,  $t = -i\tau$ . The path integral becomes

$$Z = \int \mathcal{D}g e^{-S[g]}.$$

Although the integral is performed over all metrics consistent with the boundary conditions, the presence of the minus sign in the exponential means that the integral is dominated by metrics that minimize the action, as shown in Figure 2. Wormholes are given by metrics that are usually found by solving the Einstein equations, but these solutions extremize the action, not necessarily minimize it. If a wormhole solution is a maximum of the action, it may not contribute significantly to the overall path integral. In that case, its role in the problems just described may be limited.

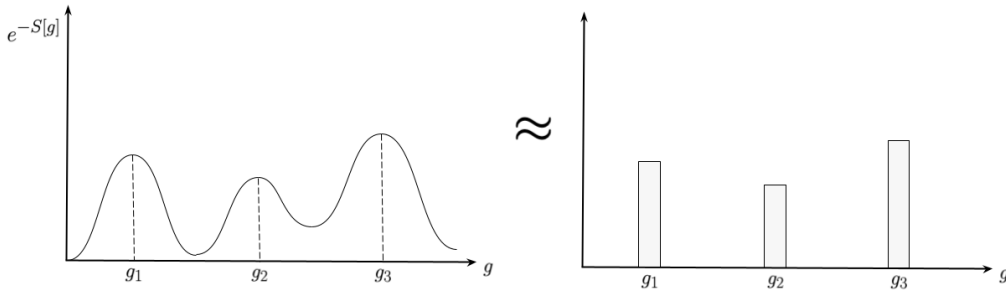


**Figure 2. The gravitational path integral is the sum over all geometries, but if the configuration space is dominated by a few points with low action, the path integral can be approximated by the sum only over those metrics.**

Another feature of wormholes that maximize the action is that they are unstable when perturbed. Determining whether a wormhole is unstable involves expressing the action in terms of fluctuations of the metric around the wormhole solution and checking whether it has negative eigenvalues. These negative modes are not expected to dominate

when integrated over nearby configurations in the path integral. In this way, understanding negative modes is crucial in assessing the importance of wormholes in quantum gravity.

The goal of this report is to describe the process of identifying negative wormhole modes in various representative gravitational models. In Section 2, a theory with three gauge fields in four-dimensional anti-de Sitter space is considered.

## 2. Einstein-Maxwell Theory with $S^3$ Boundary

This section closely follows Section 4 of [2], while elaborating on the calculations and at times supplying alternative derivations. The model consists of three Maxwell fields  $F_{\mu\nu}^i = dA^i$  in four-dimensional AdS. The action is given by

$$S = - \int_{\mathcal{M}} d^4x \sqrt{g} \left( R + \frac{6}{L^2} - \sum_{i=1}^3 F_{\mu\nu}^i F_i^{\mu\nu} \right) - 2 \int_{\partial\mathcal{M}} d^3x \sqrt{h} K + \mathcal{S}_{\mathcal{B}}, \quad (1)$$

where  $L$  is the AdS length scale,  $h$  is the determinant of the induced metric on the boundary  $\partial\mathcal{M}$ , and  $K$  is the extrinsic curvature associated with an outward-pointing normal to the boundary. The first integral is called the on-shell Euclidean action. The second term is the Gibbons-Hawking-York term needed to make the variational problem well-defined in the presence of a boundary. The final term, required to make the on-shell action finite, is given by

$$\mathcal{S}_{\mathcal{B}} = \int_{\partial\mathcal{M}} d^3x \sqrt{h} \left( \frac{4}{L} + L\mathcal{R} \right),$$

where  $\mathcal{R}$  is the intrinsic Ricci scalar on  $\partial\mathcal{M}$ .

The equations of motion derived by varying Equation 1 with respect to the metric and fields are

$$R_{\mu\nu} + \frac{3}{L^2} g_{\mu\nu} = 2 \sum_{i=1}^3 \left( F_{\mu\rho}^i F_{\nu}^{i,\rho} - \frac{g_{\mu\nu}}{4} F_{\rho\sigma}^i F_i^{\rho\sigma} \right),$$

$$\nabla_{\mu} F_i^{\mu\nu} = 0.$$

The first equation is the trace-reversed Einstein equation, where the right-hand side is the energy-momentum of the Maxwell fields. The second equation represents the covariant Maxwell equations.

To find solutions to the equations, a spherically symmetric metric is used. The metric on the round three-sphere is

$$d\Omega^2 = \frac{1}{4}(\sigma_1^2 + \sigma_2^2 + \sigma_3^2),$$

where  $\sigma_i$ , expressed in terms of Euler angles, are

$$\begin{aligned} \sigma_1 &= -\sin \psi \, d\theta + \cos \psi \sin \theta \, d\varphi, \\ \sigma_2 &= \cos \psi \, d\theta + \sin \psi \sin \theta \, d\varphi, \\ \sigma_3 &= d\psi + \cos \theta \, d\varphi, \end{aligned}$$

with  $\psi \in (0, 4\pi)$ ,  $\theta \in (0, \pi)$ , and  $\varphi \in (0, 2\pi)$ . The four-dimensional metric takes the form

$$ds^2 = \frac{dr^2}{f(r)} + g(r)d\Omega^2,$$

with  $r \in (0, \infty)$ , where  $r = \infty$  corresponds to the conformal boundary. The vector potentials are given by

$$A^i = L \frac{\sigma_i}{2} \Phi(r).$$

Both disconnected and connected, or wormhole, solutions can be constructed from the metric by appropriate choice of the function  $g$ , which represents the gauge freedom of the metric.

### 2.1. Disconnected Solutions

To find disconnected solutions, the choice  $g(r) = r^2$  is made. At  $r = 0$ , the round three-sphere smoothly shrinks to zero. With this choice, the metric becomes

$$g_{\mu\nu} = \begin{pmatrix} \frac{1}{f(r)} & 0 & 0 & 0 \\ 0 & \frac{1}{4}r^2 & 0 & \frac{1}{4}r^2 \cos \theta \\ 0 & 0 & \frac{1}{4}r^2 & 0 \\ 0 & \frac{1}{4}r^2 \cos \theta & 0 & \frac{1}{4}r^2 \end{pmatrix}.$$

The distinct Einstein equations are

$$2r^4 - L^2 r^3 f'(r) = 2L^4 \left[ r^2 f(r) \Phi'(r)^2 - 4\Phi(r)^2 \right], \quad (2)$$

$$6r^4 - L^2 r^2 \left[ r f'(r) + 4f(r) - 4 \right] = 2L^4 \left[ 4\Phi(r)^2 - r^2 f(r) \Phi'(r)^2 \right]. \quad (3)$$

The Maxwell equations reduce to

$$2r^2 f(r) \Phi''(r) + r^2 \Phi'(r) f'(r) + 2r f(r) \Phi'(r) - 8\Phi(r) = 0. \quad (4)$$

Regularity of the metric and fields requires

$$\begin{aligned} f(0) &= 1, \\ \Phi'(r) &= 0. \end{aligned}$$

With those boundary conditions, the solutions to Equations 2–4 are

$$\begin{aligned} f(r) &= 1 + \frac{r^2}{L^2}, \\ \Phi(r) &= \Phi_0 \frac{\sqrt{L^2 + r^2} - L}{\sqrt{L^2 + r^2} + L}. \end{aligned}$$

It turns out that the energy-momentum tensor is zero, and that the disconnected solutions are vacuum solutions. The on-shell Euclidean action of the solution evaluates to

$$S_D = 8\pi^2 L^2 (1 + 3\Phi_0^2). \quad (5)$$

## 2.2. Connected Solutions

Connected solutions exhibit a wormhole throat with a minimum radius  $r_0$ . To achieve this, the gauge can be set to  $g(r) = r^2 + r_0^2$ . There are two asymptotic regions, at  $r = \pm\infty$ . A global  $\mathbb{Z}_2$  symmetry relates the two spheres while leaving the minimal sphere invariant.

With the new gauge choice, the unique Maxwell equation is

$$(r^2 + r_0^2) \left[ 2f(r)\Phi''(r) + f'(r)\Phi'(r) \right] + 2rf(r)\Phi'(r) - 8\Phi(r) = 0,$$

which simplifies to

$$\frac{d}{dr} \left[ (r^2 + r_0^2) f(r) \Phi'(r)^2 - 4\Phi(r)^2 \right] = 0.$$

After integration, this becomes

$$f(r) = \frac{C + 4\Phi(r)^2}{(r^2 + r_0^2)\Phi'(r)^2}, \quad (6)$$

where  $C$  is the constant of integration. Using Equation 6, the Einstein equations are

$$\begin{aligned} 2(r^2 + r_0^2)^2 - L^2 \left[ (r^2 + r_0^2) r f'(r) + 2r_0^2 f(r) \right] &= 2CL^4, \\ 6(r^2 + r_0^2)^2 - L^2 \left[ (r^2 + r_0^2)(r f'(r) + 2f(r) - 4) + 2r^2 f(r) \right] &= -2CL^4. \end{aligned}$$

Combining these two equations yields

$$\Phi'(r)^2 - \frac{L^2 r^2 [C + 4\Phi(r)^2]}{(r^2 + r_0^2) [CL^4 + (r^2 + r_0^2)(L^2 + r^2 + r_0^2)]} = 0. \quad (7)$$

Rearranging, and again using Equation 6, results in

$$f(r) = \frac{CL^4 + (r^2 + r_0^2)(L^2 + r^2 + r_0^2)}{L^2 r^2}. \quad (8)$$

To avoid a singularity at  $r = 0$ , the integration constant must be

$$C = -\frac{L^2 r_0^2 + r_0^4}{L^4}.$$

With this choice, Equation 8 becomes

$$f(r) = \frac{L^2 + r^2 + 2r_0^2}{L^2}.$$

From Equation 7, it can be shown that the solution for  $\Phi$  is

$$\Phi(r) = \Phi_* \cosh \left[ \frac{2}{b} F \left( \arctan \left( \frac{r}{La} \right) \middle| 1 - \frac{a^2}{b^2} \right) \right], \quad (9)$$

where  $F(\phi|m)$  is the elliptic integral of the first kind.

The source of the Maxwell fields corresponds to  $\Phi(r)$  at  $r = \infty$ . Taking the  $r = \infty$  limit of Equation 9, the argument of the elliptic integral becomes  $\pi/2$ , reducing it

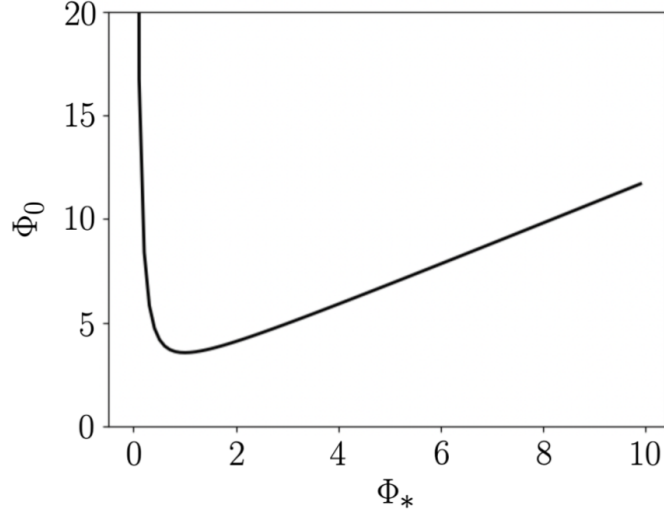


**Figure 3. The source for the Maxwell fields  $\Phi_0$  as a function of  $\Phi_*$ . There are two types of wormhole solutions for each value of  $\Phi_0$  above the minimum,  $\Phi_0^{\min}$ .**

to the complete elliptic integral of the first kind,  $K(m)$ . The source  $\Phi_0$  as a function of  $\Phi_*$  is then

$$\Phi_0(\Phi_*) = \Phi_* \cosh \left[ \frac{2}{b} K \left( 1 - \frac{a^2}{b^2} \right) \right]. \quad (10)$$

For a single value of the source  $\Phi_0$ , there can be two values of  $\Phi_*$ , as shown in Figure 3. Wormhole solutions only exist if  $\Phi_0 \geq \Phi_0^{\min} \approx 3.5633$ , which corresponds to  $\Phi_* = \Phi_*^{\min} \approx 1.0023$ . The different values of  $\Phi_*$  correspond to different wormhole solutions.

Another way of analyzing the two wormhole solutions is by studying how the radius of the wormhole throat changes with the source, as depicted in Figure 4. For  $\Phi_0$  above the minimum, there are two values of  $r_0$ , which correspond to small and large wormholes. At  $r_0^{\min} \approx 1.2515L$ , the two wormholes merge. It turns out that only the small wormhole exhibits a negative mode.

Substituting the connected wormhole solution into the on-shell Euclidean action of Equation 1, and evaluating the integral, leads to the action

$$S_C = \frac{8\pi^2 L^2}{(X-1)^{3/2}} \left[ 2(X-1)E(-X) - (X-2)K(-X) + \frac{3X}{4\sqrt{X-1}} \sinh \left( 4\sqrt{X-1}K(-X) \right) \right], \quad (11)$$

where  $X \equiv 1 + L^2/r_0^2$  and  $E(m)$  is the complete elliptic integral of the second kind. To assess whether the connected solution has a lower action than the disconnected one, Equation 11 can be subtracted from Equation 5 to produce the metric

$$\Delta S \equiv 2S_D - S_C,$$

which is plotted in Figure 5. The upper and lower branches correspond to the large and small wormhole, respectively. If  $\Delta S > 0$ , the wormhole solution has a lower action, so it

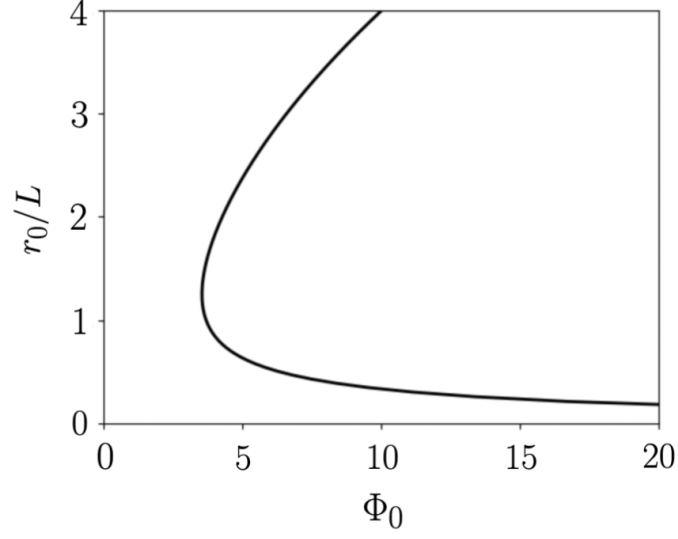


**Figure 4.** The radius of the wormhole throat  $r_0/L$  as a function of  $\Phi_0$ . For  $\Phi_0 \geq \Phi_0^{\min}$ , small and large wormholes exist.

should dominate in the path integral. The large wormhole is dominant for  $\Phi_0 \gtrsim 3.8597$ , while the small wormhole is always subdominant.

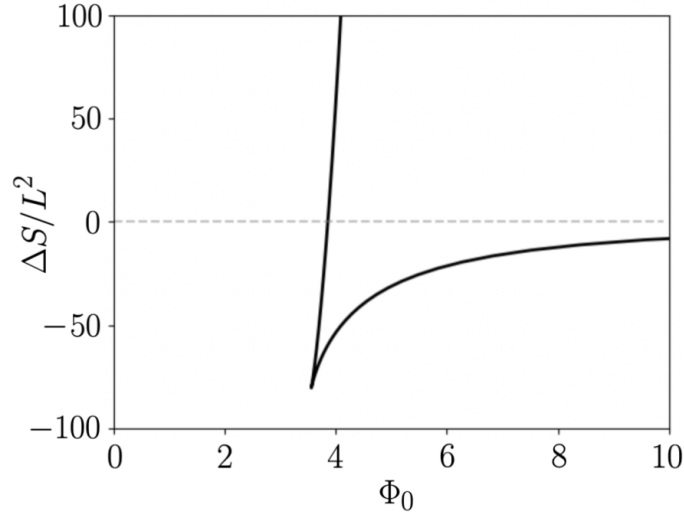


**Figure 5.** The difference in the on-shell Euclidean action between the disconnected and connected wormhole solutions. The upper branch corresponds to the large wormhole, which becomes dominant when  $\Delta S > 0$ , meaning the connected solution has a lower action.

### 2.3. Scalar Perturbations

To identify negative modes, the metric can be perturbed around the wormhole solution. There are several types of perturbations, including scalar, vector, and tensor perturbations, but this report will only focus on scalar perturbations. The metric and fields take the same

form as before, with perturbations  $\delta g$ ,  $\delta f$ , and  $\delta\Phi$  applied to the background fields as

$$\begin{aligned} g(r) &= \bar{g}(r) + \delta g(r), \\ f(r) &= \bar{f}(r) + \delta f(r), \\ \Phi(r) &= \bar{\Phi}(r) + \delta\Phi(r), \end{aligned}$$

where  $\bar{\Phi}(r)$  is given by Equation 9 and

$$\begin{aligned} \bar{g}(r) &= r^2 + r_0^2, \\ \bar{f}(r) &= \frac{L^2 + r^2 + 2r_0^2}{L^2}. \end{aligned}$$

The action is expanded to second order in the perturbations. Integrating out the angular part, the Euclidean on-shell action is

$$S_E = \frac{\pi^2}{8L^2} \int \frac{dr}{\sqrt{fg}} \left[ 12L^4 (4\Phi^2 + fg\Phi'^2) + 3L^2 (2fg'' + f'g' - 4) - 12g^2 \right],$$

where, for simplicity, the explicit dependence on  $r$  in the various functions has been removed. The variations with respect to  $\delta g$  and  $\delta f$

$$\begin{aligned} \frac{\delta S_E}{\delta g} &= -\frac{3\pi^2}{16L^2} \int \frac{dr}{\sqrt{fg^3}} \left[ 12g^2 + 16L^4\Phi^2 + L^2fg'^2 - \right. \\ &\quad \left. 2L^2g(2fg'' + 2fL^2\Phi'^2 + f'g' - 2) \right], \\ \frac{\delta S_E}{\delta f} &= \frac{3\pi^2}{16L^2} \int \frac{dr}{\sqrt{gf^3}} \left[ 4g^2 - 16L^4\Phi^2 - L^2fg'^2 + 4g(L^2 + L^4f\Phi'^2) \right] \end{aligned}$$

vanish because of the Einstein equations. The variation with respect to  $\delta\Phi$  also vanishes because of the unique Maxwell equation

$$\frac{\delta S_E}{\delta\Phi} = -\frac{3L^2\pi^2}{2} \int \frac{dr}{\sqrt{fg}} \left( fg'\Phi' + gf'\Phi' + 2fg\Phi'' - 8\Phi \right).$$

The second-order variation of the action can be decomposed into a part dependent on  $\delta g$  and  $\delta\Phi$  and their derivatives, and a part dependent on  $\delta f$  and its derivative. After integration by parts, the second part has no reliance on  $\delta f'$ . Using Equation 6, the  $f$  component of the second-order action is

$$\begin{aligned} S_f^{(2)} &= \frac{\pi^2}{32L^2} \int \frac{dr}{(\bar{g}\bar{f})^{3/2}} \left[ 12L^2\bar{g} \left( L^2\bar{g}\bar{\Phi}'^2 - 3r^2 \right) \delta f^2 - 192L^4\bar{g}\bar{\Phi}\delta f\delta\Phi + \right. \\ &\quad 48L^4\bar{f}\bar{g}^2\bar{\Phi}'\delta f\delta\Phi' + 12L^2\bar{g}\bar{f}\bar{g}'\delta f\delta g' - \\ &\quad \left. 3 \left( 16L^4\bar{\Phi}^2 + 4L^4\bar{f}\bar{g}\bar{\Phi}'^2 + L^2\bar{f}\bar{g}'^2 + 4L^2\bar{g} + 12\bar{g}^2 \right) \delta f\delta g \right]. \end{aligned}$$



This action is invariant under the infinitesimal gauge transformation  $\xi \equiv \xi_r(r)\partial_r$ . Under this transformation, a metric perturbation  $h$  and gauge field  $a$  transform as

$$\Delta h = \mathcal{L}_\xi \bar{g},$$

$$\Delta a = \mathcal{L}_\xi \bar{A},$$

where  $\mathcal{L}_\xi$  is the Lie derivative along  $\xi$ , and  $(\bar{g}, \bar{A})$  are the metric and gauge potential background fields. Notice the  $\bar{g}$  here is different than the  $\bar{g}$  above. From the definition of the Lie derivative, the perturbations transform as

$$\Delta \delta f = \xi_r \bar{f}' - 2\bar{f} \xi_r', \quad (12)$$

$$\Delta \delta g = 2r \xi_r', \quad (13)$$

$$\Delta \delta \Phi = \xi_r \bar{\Phi}'. \quad (14)$$

The transformations of the perturbation derivatives are

$$\Delta \delta g' = 2\xi_r + 2r \xi_r',$$

$$\Delta \delta \Phi' = \xi_r \bar{\Phi}'' + \xi_r' \bar{\Phi}'.$$

Using these transformations, it follows that the gauge transformation of the action,  $\Delta S_f^{(2)}$ , is zero. Since the action is gauge invariant, it is convenient to choose  $\delta g = 0$ . The action simplifies to

$$S_f^{(2)} = \frac{3\pi^2}{8} \int \frac{dr}{\sqrt{\bar{f}\bar{g}^3}} \left[ \left( L^2 \bar{g} \bar{\Phi}'^2 - 3r^2 \right) \delta f^2 - L^2 \bar{\Phi} \delta f \delta \Phi + 4L^2 \bar{g}^2 \bar{\Phi}' \delta f \delta \Phi' \right].$$

Given the algebraic dependence on  $\delta f$  in the action, the square can be completed, transforming the action into the form

$$S_f^{(2)} = \int dr \left[ - \left( a_1 \delta f + a_2 \delta \Phi + a_3 \delta \Phi' \right)^2 + C_0 \right],$$

where  $a_i$  are functions of the background fields only. The first term is a Gaussian integral that can be computed, and the result can be absorbed into the measure in the path integral. The remaining part involving  $C_0$  is given by

$$S_f^{(2)} = \frac{\pi^2}{2} \int \frac{dr}{\sqrt{\bar{g}\bar{f}^3} (r^2 - L^2 \bar{g} \bar{\Phi}'^2)} \left[ 48L^4 \bar{\Phi}^2 \delta \Phi^2 + 24L^4 \bar{f} \bar{g} \bar{\Phi} \bar{\Phi}' \delta \Phi \delta \Phi' + \right. \\ \left. 3L^4 (\bar{f} \bar{g} \bar{\Phi}')^2 \delta \Phi'^2 \right].$$

The part of the action not involving  $f$  can be expressed in terms of the gauge invariant quantity

$$q \equiv \delta \Phi - \bar{\Phi}' \frac{\delta g}{2r}.$$

Using Equations 12–14, it can be shown that  $\Delta q = 0$ . When  $\delta g = 0$ ,  $q = \delta\Phi$ . Making that simplification, the  $q$  part of the action is

$$S_q^{(2)} = \frac{3L^2\pi^2}{2} \int \frac{dr}{\sqrt{\bar{g}\bar{f}}} (4q^2 + \bar{f}\bar{g}q'^2).$$

The two parts of the action can be combined. After performing integration by parts on the  $qq'$  term, the result is

$$S^{(2)} = \frac{\pi^2}{4} \int dr \sqrt{\frac{\bar{g}}{\bar{f}}} \left[ \bar{f}Kq'^2 + Vq^2 \right],$$

where

$$K \equiv \frac{6L^2r^2}{r^2 - L^2\bar{g}\bar{\Phi}'^2},$$

$$V \equiv \frac{4K}{\bar{g}} \left[ \frac{2\bar{g}}{L^2r\bar{f}} \frac{L^2(r - L^2\bar{\Phi}\bar{\Phi}') + \bar{g}(r - 2L^2\bar{\Phi}\bar{\Phi}')}{r^2 - L^2\bar{g}\bar{\Phi}'^2} - 1 \right].$$

### 3. Appendix

The calculations in this report were performed using Python and Mathematica. The `sympy` package was used for symbolic computation, including tensor algebra. Calculations of the Ricci tensor and scalar were performed using the `einsteinpy` package. Jupyter notebooks were used to run and analyse the results. The code can be found in [3].

### References

- [1] A. Kundu, “Wormholes and Holography: An Introduction,” *The European Physical Journal C*, vol. 82, no. 5, may 2022. [Online]. Available: <https://doi.org/10.1140/epjc/s10052-022-10376-z>
- [2] D. Marolf and J. E. Santos, “AdS Euclidean wormholes,” *Classical and Quantum Gravity*, vol. 38, no. 22, p. 224002, oct 2021. [Online]. Available: <https://doi.org/10.1088/1361-6382/2fac2cb7>
- [3] J. Chryssathacopoulos. (2022) Analysis of Wormholes using Python. [Online]. Available: <https://github.com/jchryssanthacopoulos/wormholes>